

Electronic Supplementary Information

Beyond the Ordinary: Exploring the Synergistic Effects of Iodine and Nickel Doping in Cobalt Hydroxide for Superior Energy Storage Applications

Sheraz Yousaf^a, Sonia Zulfiqar^{b,c}, Muhammad Usman Khalid^a, Muhammad Farooq Warsi^{a*}, Imran Shakir^d, Muhammad Shahid^e, Iqbal Ahmad^{f*}, Eric. W. Cochran^{c,*}

^a*Institute of Chemistry, Baghdad-ul-Jadeed Campus, The Islamia University of Bahawalpur, Bahawalpur, - 63100, Pakistan*

^b*Department of Chemistry, Faculty of Science, University of Ostrava, 30. Dubna 22, Ostrava 701 03, Czech Republic*

^c*Department of Chemical and Biological Engineering, Iowa State University, Sweeney Hall, 618 Bissell Road, Ames, Iowa 50011, United States*

^d*Department of Physics, Faculty of Science, Islamic University of Madinah, Madinah 42351, Saudi Arabia*

^e*Department of Chemistry, College of Science, University of Hafr Al Batin, P. O. Box 1803, Hafr Al Batin, 31991, Saudi Arabia*

^f*Department of Chemistry, Allama Iqbal Open University, Islamabad, 44000, Pakistan*

Corresponding authors: (farooq.warsi@iub.edu.pk), (Iqbal.ahmad@aiou.edu.pk), (ecochran@iastate.edu)

Characterization

The structural characterization of the material was conducted using a Lab XRD-6100 diffractometer and an IR Affinity-1s spectrophotometer. The morphology and chemical composition of the material was tested using ZEISS LEO SUPRA 55 and JEOL JCM-6000Plus SEM, respectively. The XPS measurements were performed using a Kratos Amicus/ESCA 3400 instrument. The sample was irradiated with 240 W unmonochromated Mg K α X-rays, and photoelectrons emitted at 0° from the surface normal were energy analyzed using a DuPont type analyzer. The pass energy was set at 150 eV. CasaXPS was used to process raw data files. TEM images were recorded using JEOL JSM 2100 transmission electron microscope operating at 200kV.

For the electrochemical studies, a Gamry 5000E potentiostat was used, with a 3-electrode system consisting of a platinum wire counter electrode, an Hg/HgO reference electrode, and a

CFC-based modified working electrode in 1 M KOH-aqueous-solution. The potentials were converted to RHE using the following equation:

$$E_{RHE} = E_{Hg/HgO} + 0.059 \text{ pH} + E_{Hg/HgO}^{\circ}$$

The following equations were used to find essential parameters

The power law is given as

$$\text{Log (I)} = b \text{log}(v) + \text{log (a)} \tag{Eq. ES1}$$

Where I represent anodic or cathodic peak current at fixed scan rate (v) and b is kinetic constant. The Dunn method for determining the percent contribution for diffusion and the capacitive process is calculated as.

$$\frac{i}{v^{\frac{1}{2}}} = k_1 v + k_2 v^{\frac{1}{2}} \tag{Eq. ES2}$$

Where, i represents current at fixed potential V, $k_1 v$ and $k_2 v^{\frac{1}{2}}$ represents $i_{\text{capacitive}}$ and $i_{\text{diffusivity}}$. Where I and t are denoted as current and discharging time.

$$C_{\text{sp}} = \frac{\int I dt}{m \Delta V} \tag{Eq. ES3}$$

Where, I and t are denoted as current and discharging time. The specific capacitance values in F/g were converted to specific capacity (C/g) by multiplying it with potential window. The determination of the turnover frequency (TOF) involves the use of mathematical expression.

$$\text{TOF} = \frac{J \times A}{4 \times F \times n} \tag{Eq. ES4}$$

The aforementioned equation establishes a correlation between J, which denotes the electric current per unit area of the electrode surface, and A, which represents the exposed surface area of the electrode. The constant F is used to establish the correlation between the quantity of

charge and the overall number of moles of electrolytes that participate in a redox reaction. The value of F is approximately equivalent to 96,485 coulombs per mole. Moreover, the variable "n" denotes the overall quantity of metallic elements contained within the substance [1].

Preparation of electrode material

In the current experiment, a premeasured size of activated carbon fiber cloth was taken and washed thoroughly with deionized water, ethanol, and acetone to remove any impurities or contaminants. Next, a mixture of catalysts (15 mg) and distilled water (100 μL) was sonicated for 2 hours to create an ink. This ink was then drop-cast onto selected regions of the CFC to form an electrode. The resulting electrode was used as a working electrode in the subsequent electrochemical analysis. Overall, these steps ensured the electrode was properly prepared and ready for use in the study.

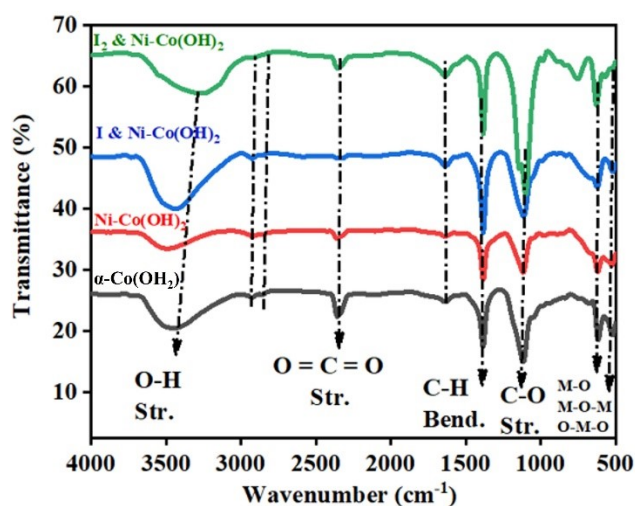


Figure ES1. FTIR spectra of $\alpha\text{-Co(OH)}_2$, Ni-doped- Co(OH)_2 , I & Ni-co-doped- Co(OH)_2 , and I_2 -loaded Ni-doped- Co(OH)_2 electrocatalysts.

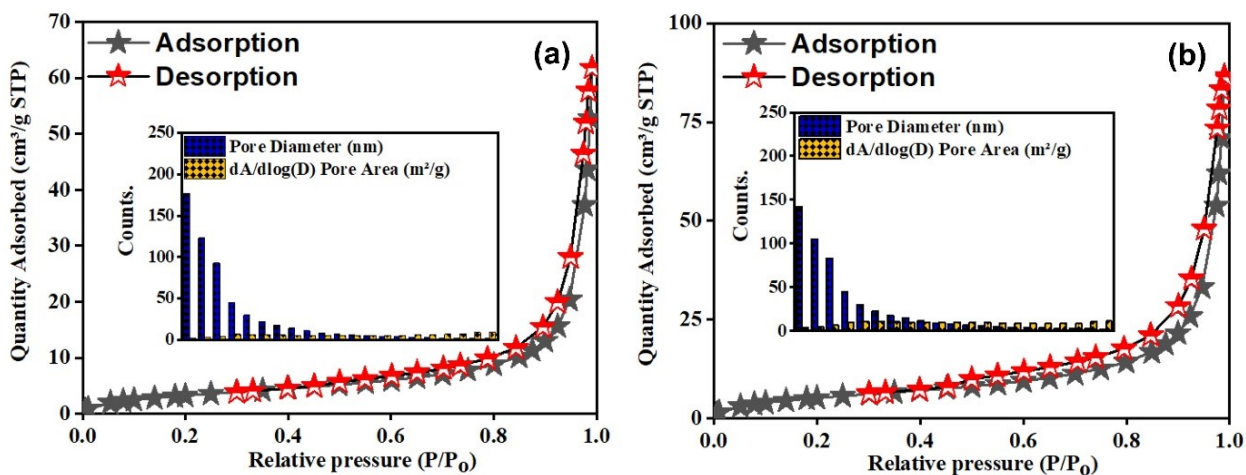


Figure ES2. BET plots for (a) Ni-doped-Co(OH)₂, (b) I & Ni-co-doped Co(OH)₂ electrocatalysts. The inset shows the bar-graphs representing pore diameter and pore area.

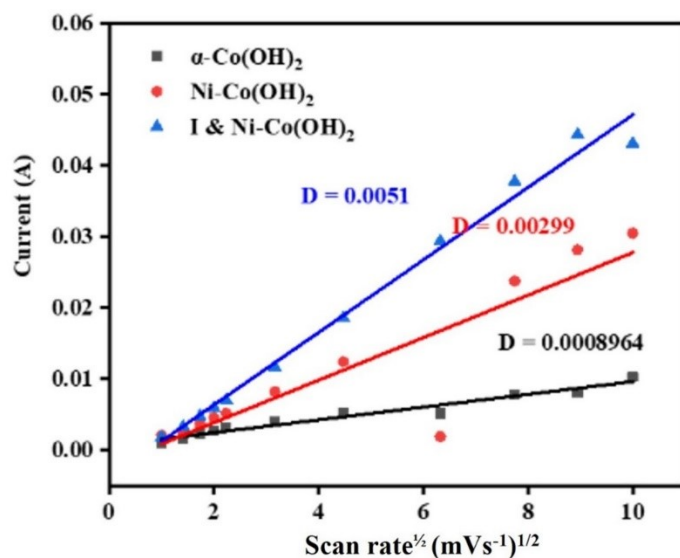


Figure ES3. Graphical representation of relation between peak current to the square root of the scan rate

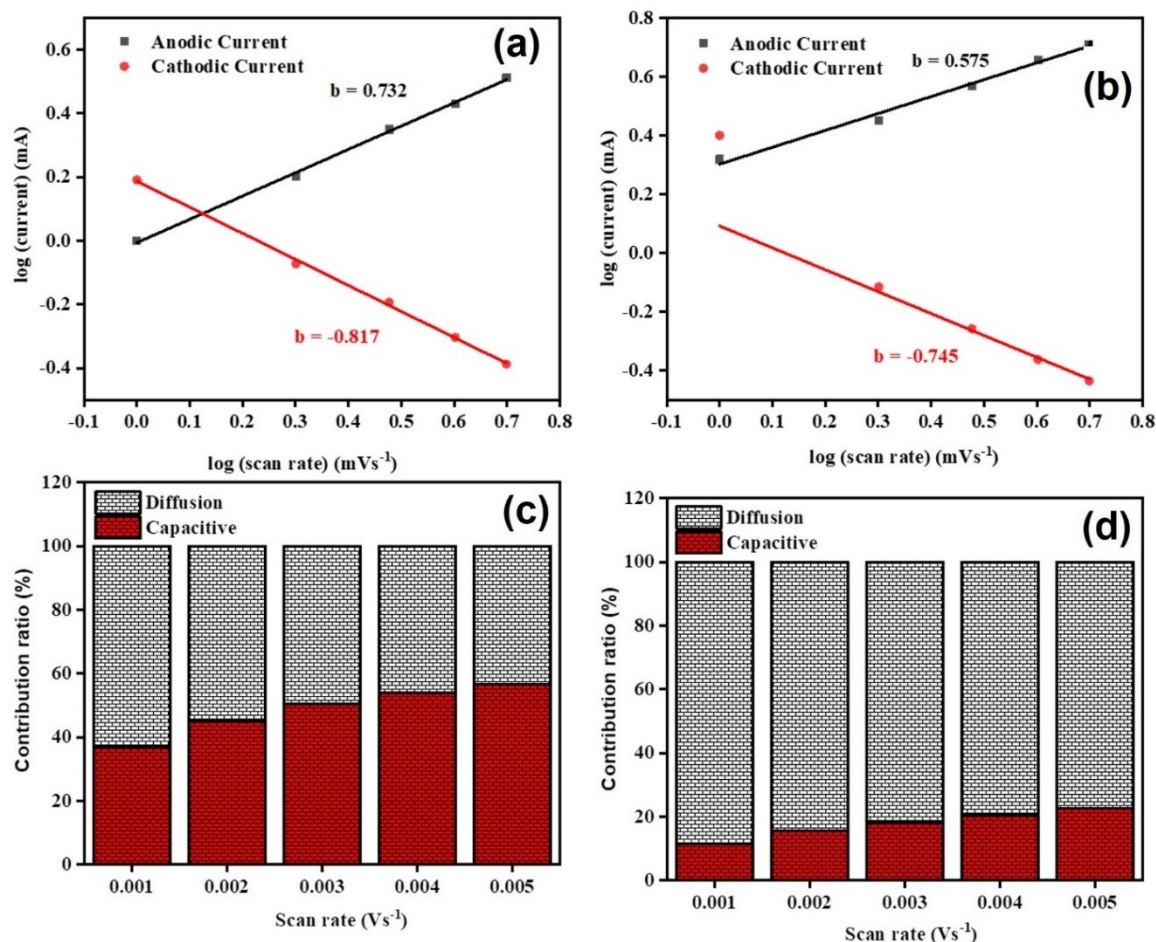


Figure ES4. Graph showing relationship between anodic and cathodic peak currents vs logarithm of the scan rate for α -Co(OH)₂ (a) Ni-doped-Co(OH)₂ (b). The percentage contribution of capacitive and diffusion controlled processes for α -Co(OH)₂ and Ni-doped-Co(OH)₂ “c” and “d”.

Electrochemically active surface area

In the analysis of electrocatalytic sites positioned at the interface of the electrode and electrolyte, it is essential to consider the electrochemically active surface area (ECSA). Accurate calculation of this parameter is crucial in the assessment of electrocatalytic performance. Taking advantage of the electrical double layer capacitance (EDLC) technique, which is a popular approach, in determining the electrochemically active surface area (ECSA) of particular electrocatalysts [2]. The electrocatalytic activity of an electrocatalyst can be significantly enhanced by increasing its surface area. The present investigation involved the determination of the electrochemically active surface area (ECSA) of the synthesized electrocatalysts, namely α -Co(OH)₂, Ni-doped-Co(OH)₂, and I & Ni co-doped-Co(OH)₂, through the application of the EDLC technique. Cyclic voltammetry (CV) data were obtained at different scan rates across a potential range where the current was believed to be induced by a charging electrical double layer. Table ES1 presents the ECSA values of the electrocatalysts.

The findings indicate that the electrocatalysts α -Co(OH)₂ co-doped with I and Ni exhibited a greater effective catalytic surface area in comparison to the pure electrocatalysts. The observed phenomenon can be ascribed to the amplified surface area and porous morphology of the substance, which may improve the availability of the located active sites. The enhanced electrocatalytic performance for OER and HER can be ascribed to a synergistic influence. Figure ES5 presents the cyclic voltammetry plots of the electroactive substances under varying scan rates.

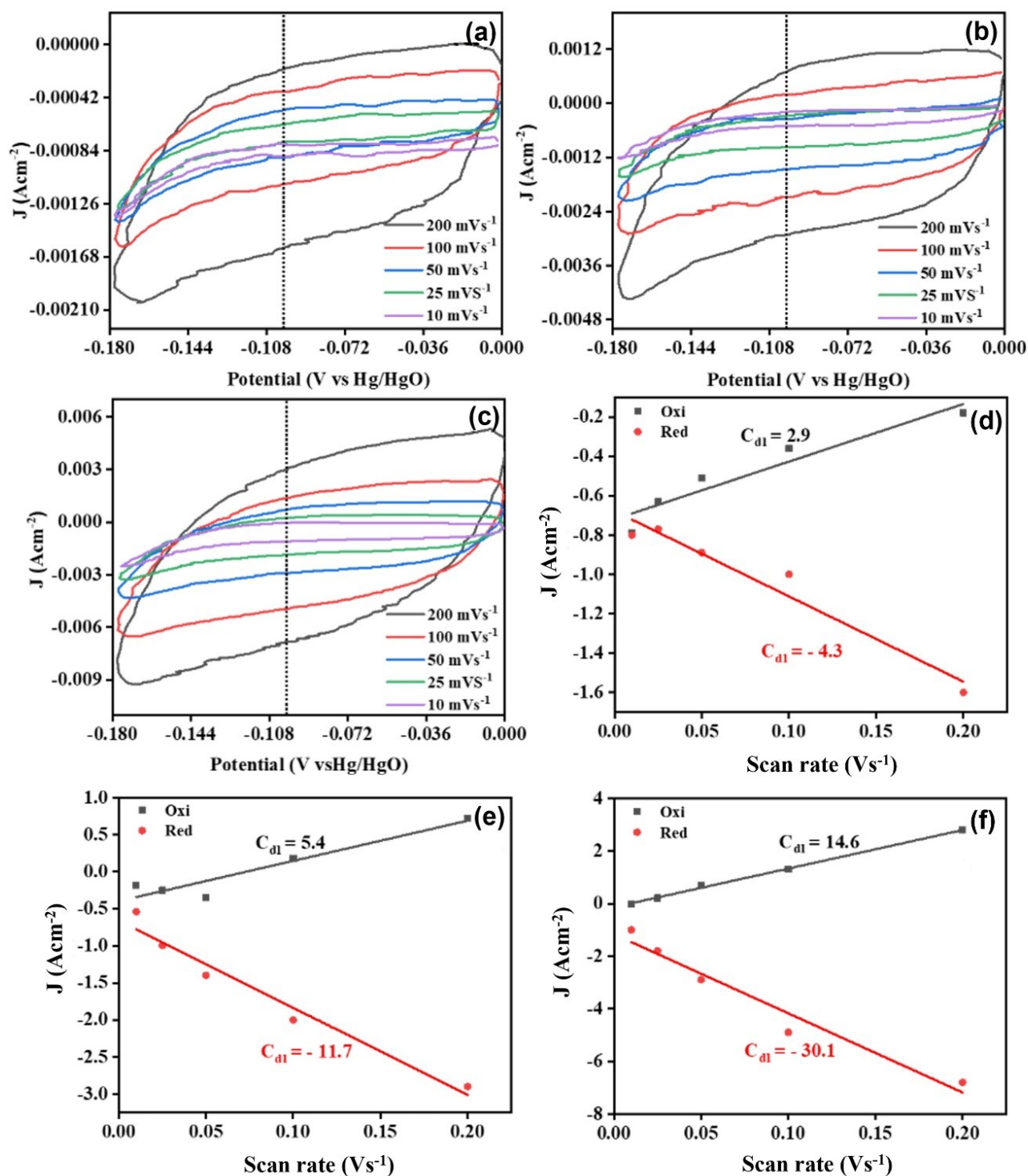


Figure ES5. Electrochemical active surface area for (a) α -Co(OH)₂ (b) Ni-doped-Co(OH)₂ and (c) I & Ni-co-doped-Co(OH)₂.

The quantification of active sites available for the electrolyte in the electrocatalyst is directly correlated with the charge covering the reduction peak that is apparent in the voltammogram. The electrocatalysts that have been synthesized can be evaluated in terms of their electrochemical accessibility by measuring the charge contained within the reduction peak.

This measurement is conducted at a low scan rate of 20 mVs⁻¹. The reduction peak's enclosed charge was determined by analyzing the chemical adsorption of a single oxygen atom onto a singular nickel or cobalt atom, utilizing the redox couple as a reference [3]. Of all the electrocatalysts examined within current study, the I & Ni-co-doped-Co(OH)₂ exhibited a greater quantity of charge comprised by the reduction peak, suggesting superior electrochemical accessibility. The authors calculated the atomic surface concentration of the I & Ni-co-doped-Co(OH)₂ electrocatalysts using the charge controlled by the redox couple. The atomic surface concentration of the co-doped electrocatalysts was found to be greater than that of the pristine electrocatalysts.

Table ES1. Preliminary electrochemical experimental parameters for α -Co(OH)₂, Ni-doped-Co(OH)₂, and I & Ni co-doped-Co(OH)₂.

S. No.	Material	C _{dL} (cm ⁻²)	ECSA (cm ²)	The surface concentration of atoms ($\times 10^{18}$)	Exchange Current density (mAcm ⁻²)
1	α -Co(OH) ₂	4.6	90	1.69	0.95
2	Ni-Co(OH) ₂	8.6	214	3.44	1.78
3	I & Ni-Co(OH) ₂	22.4	560	3.93	2.67

Table ES2. Comparative studies of the I & Ni-co-doped-Co(OH)₂ electrocatalyst in terms of OER and HER performance with previously reported literature.

Electrocatalyst	Electrolyte	Method of synthesis	Overpotential (mV) at 10 mA cm ⁻²		Tafel slope (mVdec ⁻¹)		Ref
			OER	HER	OER	HER	
Mo-Ni(OH) ₂ /Fe _x Ni _y (OH) _{3x+2y}	NaOH	Hydrothermal method	229	57	--	--	[4]
Mo-Co(OH) ₂ /Co ₃ O ₄ /NF-800	1 M KOH	Electrodeposition(1 st)-pyrolysis-Electrodeposition(2 nd) strategy	234	116	--	--	[5]
Ni-M@C-130		Partial sulfurization strategy	244 @ η ₁₀	123 @ η ₁₀	47.2	50.8	[6]
CeCO ₃ OH/Ce-CoFe LDH		One-step hydrothermal process	216	165	--	--	[7]
Ce-Co(OH) ₂ /CoP/NF		Hydrothermal process	253	56	--	--	[8]
NiS-MoS ₂ HNSAs/CC		Surfactant based material design	203 @ η ₁₀	106 @ η ₁₀	77.4	56.7	[9]
S-Ni(Fe)OOH		--	198	22	17.5	93.21	[10]
MnNiCoP/FeO OH		Electrodeposition phosphating	η ₁₀₀ =251	η ₁₀₀ =124	--	--	[11]
Zn-NiS-3		Hydrothermal technique	320 @ η ₅₀	208 @ η ₁₀	36	115	[12]
CoNiP/CoNiFeP@NCNFs		Ion exchange strategy	260	177	--	--	[13]
Ru _{SAs} /Ni(OH) ₂ @FeOOH		Hydrothermal and immersion methods	η ₁₀₀₀ =386	η ₁₀₀₀ =267	--	--	[14]
NiS@CoFeMoO ₄ /NF		Hydrothermal method	200	72	63	45	[15]
FeCoNiN/NF		Hydrothermal method	η ₅₀ =267	56	--	--	[16]
Ni ₂ O ₂ (OH)/CNTs		Ultrasonication method	η ₄₀ =228	η ₄₀ =368	132	115	[17]
Co(OH) ₂ /NF		Hydrothermal method	230	150	43	64	[18]

β -Ni(OH) ₂ /NF	Hydrothermal etching method	$\eta_{50}=329$	$\eta_{50}=170$	40	51	[19]
Ni _x Co _{1-x} (OH) ₂ /NiFe-AM	Hydrothermal and electrodeposition methods	103	157	--	--	[20]
(Ni-Fe) _x S _y /NiFe(OH) ₂	One-step electron-induced co-deposited strategy	$\eta_{100}=290$	$\eta_{100}=124$	--	--	[21]
Mo-NiS@NiFe LDH/NF	<i>In-situ</i> growth method	184	107	--	--	[22]
Ni ₃ S ₂ @Co(OH) ₂	Hydrothermal and electrodeposition methods	257	110	--	--	[23]
I & Ni-Co(OH) ₂	Precipitation route	$\eta_{40}=240$	229	188	110	This work

References

- [1] K. Xiang, J. Guo, J. Xu, T. Qu, Y. Zhang, S. Chen, P. Hao, M. Li, M. Xie, X. Guo, W. Ding, Surface Sulfurization of NiCo-Layered Double Hydroxide Nanosheets Enable Superior and Durable Oxygen Evolution Electrocatalysis, *ACS Applied Energy Materials*, 1 (2018) 4040-4049.
- [2] S. Watzele, P. Hauenstein, Y. Liang, S. Xue, J. Fichtner, B. Garlyyev, D. Scieszka, F. Claudel, F. Maillard, A.S. Bandarenka, Determination of Electroactive Surface Area of Ni-, Co-, Fe-, and Ir-Based Oxide Electrocatalysts, *ACS Catalysis*, 9 (2019) 9222-9230.
- [3] N.-U.-A. Babar, K.S. Joya, Spray-Coated Thin-Film Ni-Oxide Nanoflakes as Single Electrocatalysts for Oxygen Evolution and Hydrogen Generation from Water Splitting, *ACS Omega*, 5 (2020) 10641-10650.
- [4] Y. Liu, M. Ding, Y. Qin, B. Zhang, Y. Zhang, J. Huang, Crystalline/Amorphous Mo-Ni(OH)₂/Fe_xNi_y(OH)_{3x+2y} hierarchical nanotubes as efficient electrocatalyst for overall water splitting, *Journal of Colloid and Interface Science*, 657 (2024) 219-228.
- [5] H. Yang, T. Hu, R. Meng, L. Guo, Efficient Mo-Co(OH)₂/Co₃O₄/Ni foam electrocatalyst for overall water splitting, *Journal of Solid State Chemistry*, 320 (2023) 123837.
- [6] K. Srinivas, Y. Chen, X. Wang, B. Wang, M. Karpuraranjith, W. Wang, Z. Su, W. Zhang, D. Yang, Constructing Ni/NiS Heteronanoparticle-Embedded Metal-Organic Framework-Derived Nanosheets for Enhanced Water-Splitting Catalysis, *ACS Sustainable Chemistry & Engineering*, 9 (2021) 1920-1931.
- [7] J. Tang, J. Hu, X. Chen, B. Yang, K. Zhang, Y. Li, Y. Yao, S. Zhang, Boosting activity on CoFe layered double hydroxide by doping and heterostructure as a bifunctional electrocatalyst for efficient overall water splitting, *Fuel*, 365 (2024) 131128.
- [8] C. Lyu, J. Cheng, K. Wu, J. Wu, J. Hao, Y. Chen, H. Wang, Y. Yang, N. Wang, W.-M. Lau, J. Zheng, Interface and cation dual-engineering promoting Ce-Co(OH)₂/CoP/NF as bifunctional electrocatalyst toward overall water splitting coupling with oxidation of organic compounds, *Journal of Alloys and Compounds*, 934 (2023) 167942.
- [9] S. Guan, X. Fu, Z. Lao, C. Jin, Z. Peng, NiS-MoS₂ hetero-nanosheet array electrocatalysts for efficient overall water splitting, *Sustainable Energy & Fuels*, 3 (2019) 2056-2066.

- [10] Q. Li, B. Chen, L. Huang, S. Zhu, Y. Qian, D. Wu, S. Luo, A. Xie, S-doped Ni(Fe)OOH bifunctional electrocatalysts for overall water splitting, *International Journal of Hydrogen Energy*, 51 (2024) 1392-1406.
- [11] L. Zhu, R. Wang, X. Liu, S. Yang, H. Liu, B. Xing, K. Wang, Three-dimensional heterostructured MnNiCoP/FeOOH cross-linked nano-flake supported by Ni Foam as a bifunctional electrocatalysts for overall water splitting, *Applied Surface Science*, 656 (2024) 159711.
- [12] C. Prakash, P. Sahoo, R. Yadav, A. Pandey, V.K. Singh, A. Dixit, Nanoengineered Zn-modified Nickel Sulfide (NiS) as a bifunctional electrocatalyst for overall water splitting, *International Journal of Hydrogen Energy*, 48 (2023) 21969-21980.
- [13] L. Zhi, M. Zhang, J. Tu, M. Li, J. Liu, Coordination polymer and layered double hydroxide dual-precursors derived polymetallic phosphides confined in N-doped hierarchical porous carbon nanoflower as a highly efficient bifunctional electrocatalyst for overall water splitting, *Journal of Colloid and Interface Science*, 659 (2024) 82-93.
- [14] B. Wang, H. Sun, M. Chen, T. Zhou, H. Zheng, M. Zhang, B. Xiao, J. Zhao, Y. Zhang, J. Zhang, Q. Liu, Ru single-atom regulated Ni(OH)₂ nanowires coupled with FeOOH to achieve highly efficient overall water splitting at industrial current density, *Chemical Engineering Journal*, 479 (2024) 147500.
- [15] D. Thiagarajan, A. Thirumurugan, B.-K. Lee, Construction of NiS@CoFeMoO₄/NF nanosheet heterostructures for efficient overall water splitting, *Journal of Alloys and Compounds*, 936 (2023) 168340.
- [16] Z. Wang, S. Jiao, B. Wang, Y. Kang, W. Yin, X. Lv, Q. Zhang, Z. Zhang, Y. Chen, G. Pang, In-situ growth of Fe-Co Prussian-blue-analog nanocages on Ni(OH)₂/NF and the derivative electrocatalysts with hierarchical cage-on-sheet architectures for efficient water splitting, *International Journal of Hydrogen Energy*, 46 (2021) 8345-8355.
- [17] M. Afaq, A. BaQais, E.W. Cochran, S. Zulfiqar, M.A. Amin, M. Shahid, I. Ahmad, S. Yousaf, M.F. Warsi, Fabrication of Ni₂O₂(OH)/CNTs-based electrocatalyst for efficient bifunctional electrocatalytic water splitting, *International Journal of Hydrogen Energy*, 60 (2024) 601-610.
- [18] M. Duraivel, S. Nagappan, K.H. Park, K. Prabakar, Hierarchical 3D flower like cobalt hydroxide as an efficient bifunctional electrocatalyst for water splitting, *Electrochimica Acta*, 411 (2022) 140071.
- [19] J.-H. Yang, X. Xu, M. Chen, D. Yang, H. Lu, Y. Sun, C. Shao, Q. Song, J. Zhang, L. Gao, Y. Zhang, Morphology-controllable nanocrystal β-Ni(OH)₂/NF designed by hydrothermal etching method as high-efficiency electrocatalyst for overall water splitting, *Journal of Electroanalytical Chemistry*, 882 (2021) 115035.
- [20] J. Yu, B. Li, Z. Rao, Hydrogen production via highly efficient electrocatalyst based on 3D Ni_xCo_{1-x}(OH)₂/NiFe-AM induce overall water splitting, *International Journal of Hydrogen Energy*, 46 (2021) 29916-29925.
- [21] Q. Che, Q. Li, Y. Tan, X. Chen, X. Xu, Y. Chen, One-step controllable synthesis of amorphous (Ni-Fe)_x/NiFe(OH)_y hollow microtube/sphere films as superior bifunctional electrocatalysts for quasi-industrial water splitting at large-current-density, *Applied Catalysis B: Environmental*, 246 (2019) 337-348.
- [22] S. Qiu, B. Zhang, X. Wang, J. Huang, G. Zhao, M. Ding, X. Xu, Interface strong-coupled 3D Mo-NiS@Ni-Fe LDH flower-cluster as exceptionally efficient electrocatalyst for water splitting in wide pH range, *Journal of Colloid and Interface Science*, 641 (2023) 277-288.
- [23] S. Wang, L. Xu, W. Lu, Synergistic effect: Hierarchical Ni₃S₂@Co(OH)₂ heterostructure as efficient bifunctional electrocatalyst for overall water splitting, *Applied Surface Science*, 457 (2018) 156-163.